Appl Phys B (2010) 100: 505–514
DOI 10.1007/s00340-010-3944-7

Applied Physics B
Lasers and Optics

Atomic frequency offset locking in a Λ type three-level Doppler broadened Cs system

Y.B. Kale · A. Ray · R. D'Souza · Q.V. Lawande · B.N. Jagatap

Received: 9 November 2009 / Revised version: 18 January 2010 / Published online: 19 March 2010

Abstract We here present a comparative study of frequency stabilities of pump and probe lasers coupled at a frequency offset generated by coherent photon-atom interaction. Pump-probe spectroscopy of the Λ configuration in D_2 transition of cesium is carried out to obtain sub-natural ($\sim$2 MHz) electromagnetically induced transparency (EIT) and sub-Doppler ($\sim$10 MHz) Autler-Townes (AT) resonance. The pump laser is locked on the saturated absorption spectrum (SAS, $\sim$13 MHz) and the probe laser is successively stabilized on EIT and AT signals. Frequency stabilities of pump and probe lasers are calculated in terms of Allan variance $\sigma(2,\tau)$ by using the frequency noise power spectrum. It is found that the frequency stability of the probe stabilized on EIT is superior ($\sigma \sim 2\times10^{-13}$) to that of SAS locked pump laser ($\sigma \sim 10^{-12}$), whereas the performance of the AT stabilized laser is inferior ($\sigma \sim 6\times10^{-12}$). This contrasting behavior is discussed in terms of the theme of conventional master-slave offset locking scheme and the mechanisms underlying the EIT and sub-Doppler AT resonances in a Doppler broadened atomic medium.

Y.B. Kale · A. Ray (✉)
Laser & Plasma Technology Division, Bhabha Atomic Research Centre, Mumbai 400 085, India
e-mail: ayan_ray_in@rediffmail.com

R. D'Souza · B.N. Jagatap
Atomic and Molecular Physics Division, Bhabha Atomic Research Centre, Mumbai 400 085, India

B.N. Jagatap
e-mail: bnj@barc.gov.in

Q.V. Lawande
Theoretical Physics Division, Bhabha Atomic Research Centre, Mumbai 400 085, India

B.N. Jagatap
Homi Bhabha National Institute, Bhabha Atomic Research Centre, Mumbai 400 085, India

1 Introduction

Precision spectroscopy in coherently prepared atomic medium has received considerable attention, both theoretical and experimental, in recent years. In this context the coherent population trapping (CPT) [1] and electromagnetically induced transparency (EIT) [2], which rely on quantum mechanical interference in coherently driven three-level systems, have been investigated in several works [1–10]. Both CPT and EIT afford sub-natural frequency resolution even in an inhomogeneously broadened atomic medium, and that makes them attractive for several applications which include for example, atomic frequency standard [6], miniaturized atomic clock [7], ultra-sensitive magnetometry [8] and frequency offset locking [9, 10]. Experimentally these and other related issues are explored in alkali atoms where a suitable three-level system is constructed from the hyperfine manifolds of D_1 or D_2 transitions. Different techniques like two independent lasers [9, 10], two independent but phase locked lasers [3] and sidebands of a single laser [11] are employed to generate necessary bichromatic field in these experiments. Apart from CPT and EIT, the other consequences of the coherent interaction between a bichromatic field and atomic medium are Autler-Townes (AT) splitting [12] and related sub-Doppler absorption [13, 14] in the presence of a far detuned pump laser. Some of these works [12, 14] focus on reducing the line widths of these dressed level signals to the level of natural line width and hint on the prospective use of such resonances as precision frequency reference for laser frequency stabilization.

In general the experimental arrangements of coherent pump-probe spectroscopy that utilizes two independent lasers [9, 10] are potentially useful for developing schemes for frequency offset locking. This type of application, however, requires addressing the central issue, which concerns the stability of such frequency offset coupled laser systems. Interestingly in an offset locking scheme based on EIT, Moon et al. [9] have shown quantitatively higher frequency stability of the probe laser compared to the pump laser. This observation is in contradiction with the expected outcome of a conventional offset locking [15], where one expects the pump laser to decide the stability of the probe. It is therefore important to investigate the coherent spectroscopy based atomic frequency offset locking schemes to draw a general conclusion on the stability of the probe laser.

In this paper we report specific case study of the probe laser frequency stability while locked on EIT and sub-Doppler dressed level resonance. Three-level system used in this work is Λ configuration of the hyperfine levels of cesium D_2 transition at ~852 nm having natural line width of 5.3 MHz. The issues relating to the coherent dephasing and background absorption concerning this transition in the context of CPT like experiments have been discussed in the literature [3]. We obtain an EIT signal of line width ~2 MHz and a sub-Doppler dressed level resonance of line width ~10 MHz and use these as frequency reference for probe laser stabilization. Our experiments consist of extraction of third derivative signals of EIT and sub-Doppler absorption using frequency modulation spectroscopy (FMS). The slope of the third derivative discriminator signal is used for frequency locking. The frequency stability of the probe laser is extracted through Allan variance and is compared with that of the pump laser. We explicitly demonstrate here that the pump laser, which dresses the atomic medium, sets a limit to the frequency stability of the probe laser when locked on sub-Doppler dressed level absorption (AT) signal. On the other hand the probe laser stability can surpass that of the pump laser in case of EIT locking. This contrasting behavior is explained in terms of the very mechanism underlying EIT and sub-Doppler dressed level resonances in a Doppler broadened atomic medium.

2 Role of coherently driven Λ system in offset locking

The Λ type atomic level scheme has been studied extensively in connection with EIT, CPT and sub-Doppler dressed level resonances. Ideally a Λ system has zero coherent dephasing rate and hence capable of producing narrowest EIT signal in comparison with V or Ξ type configuration [16]. The level scheme used in our work is shown in Fig. 1, where a strong pump laser of frequency ω_1 dresses the transition $|1\rangle \rightarrow |2\rangle (6s_{1/2}F = 4 \rightarrow 6p_{3/2}F' = 3)$ and a weak probe of frequency ω_2 is scanned in the vicinity of $|3\rangle \rightarrow |2\rangle (6s_{1/2}F = 3 \rightarrow 6p_{3/2}F' = 3)$ transition.

An overall idea about Λ system is necessary to understand its influence on the frequency offset locking. Due to the coherent pump-probe interaction the susceptibility (χ) of the atomic medium is modified and following Banacloche et al. [17], we may write

$$\chi(v)dv = \frac{4i\hbar\Omega_2^2/\varepsilon_0}{\Gamma_{12} - i\Delta_1 - i\frac{\omega_2}{c}v + \frac{\Omega_1^2}{4}\left[\Gamma_{23} - i(\Delta_1 - \Delta_2) - i(\omega_2 - \omega_1)\frac{v}{c}\right]^{-1}} N(v)dv \tag{1}$$

where $\Delta_1 = \omega_1 - \omega_{21} (\Delta_2 = \omega_2 - \omega_{23})$ and $\Omega_1 (\Omega_2)$ are detuning and Rabi frequency of pump (probe) laser, Γ_{ij} is the population decay rate for $|i\rangle \rightarrow |j\rangle$ transition and $N(v)$ is the Maxwell-Boltzmann velocity distribution of the Doppler broadened atomic system. The probe laser absorption coefficient (α) is then proportional to Im(χ). Equation (1) contains all the necessary dependence of the probe absorption on the intensity and detuning of the pump laser.

When $(\omega_2 - \omega_1)/\omega_0 \ll 1$ where ω_0 is the nominal frequency of the atomic transition (852 nm for Cs D_2 transition) and $\Omega_1 \gg \Omega_2$, the probe absorption spectrum splits into the AT doublet [18] as a result of the dressing of the transition $|1\rangle \rightarrow |2\rangle$ by the pump laser. The frequency ($\delta_\pm$) and line width ($\gamma_\pm$) of these dressed level resonances in a real atomic medium with Doppler width 'D' are given by

$$\delta_\pm = \frac{1}{2}\left[\Delta_1 \pm \sqrt{\Delta_1^2 + \Omega_1^2}\right],$$
$$\gamma_\pm = \frac{\Gamma_{21} + \Gamma_{23} + 2D}{4}\left(1 \mp \frac{\Delta_1}{\sqrt{\Delta_1^2 + \Omega_1^2}}\right) \tag{2}$$

The possibility of generating a dressed level resonance of Sub-Doppler or even sub-natural line width [12–14] is contained in (1). Such narrow line width resonance can be used for the purpose of frequency stabilization. In the present work we choose the AT frequency reference obtained when the pump laser is sufficiently far blue detuned so that the sub-Doppler dressed level absorption signal appears outside the Doppler profile of Cs vapor. This scheme is advantageous since it requires simple experimental arrangement involving co-propagating pump-probe lasers, which is very

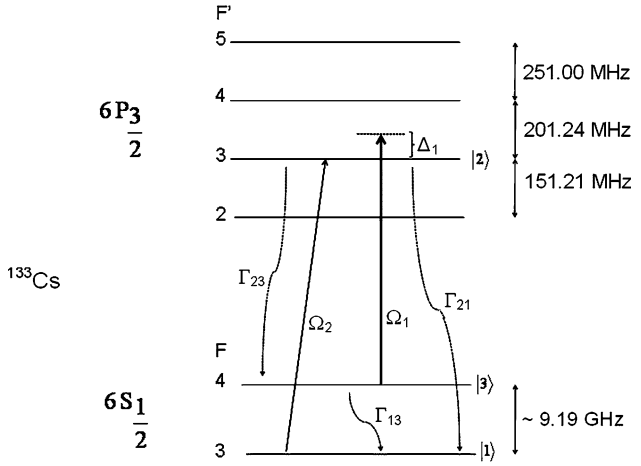

Fig. 1 Level scheme in D_2 transition of cesium atom. The relevant hyperfine levels used for pump probe spectroscopy are denoted by $|1\rangle$, $|2\rangle$ and $|3\rangle$. The Rabi frequencies of pump and probe are Ω_1 and Ω_2, and the detuning of the pump is Δ_1. The radiative decay rates for $|2\rangle \rightarrow |1\rangle$ and $|2\rangle \rightarrow |3\rangle$ are Γ_{21} and Γ_{23}, whereas Γ_{13} denotes the non-radiative decay rate

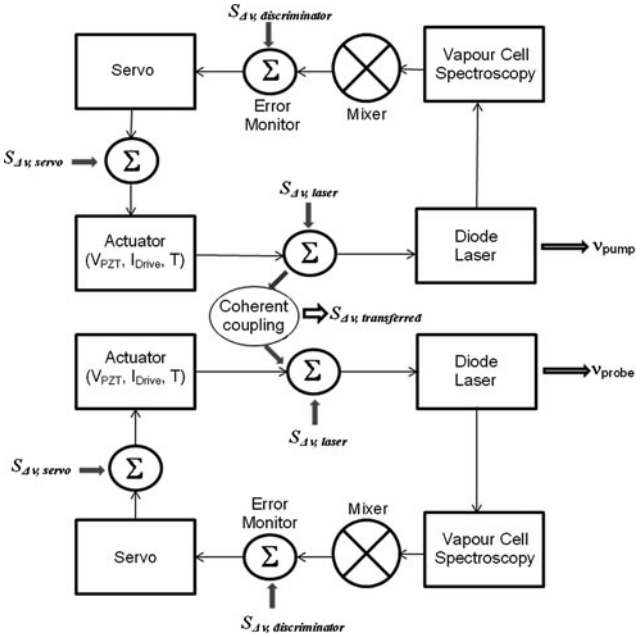

Fig. 2 Schematic representation of atomic frequency offset locking scheme. Here different elements in the control loop are assumed to be noise free. Noise $S\Delta\nu$ is introduced from outside following the convention of Ref. [19]. However for simplicity it is assumed that discriminator noise is negligible. The contribution of $S_{\Delta\nu,\text{laser}}$, laser is considered for further analysis

similar to that used in EIT experiments. Further for suitably large Δ_1 the line width of the sub-Doppler absorption signal can be reduced to the level of natural line width [12–14]. On the other hand if one chooses to use the narrow AT signal that lies in the Doppler profile (obtained with small Δ_1) then one needs to implement SAS like arrangement (co- and counter-propagating probe beams) to retrieve AT signal from the Doppler background [12] and that makes the contrast of the AT signal critically dependent on the optical alignment. This scheme may further influence the transfer function $H(f)$ of the feedback control loop, which is used to compensate probe laser frequency drift.

We now consider the case of frequency offset locking with EIT, which is a non-absorptive two-photon resonance in contrast to the dressed level resonance discussed above. EIT appears as a result of destructive interference between probability amplitudes of alternate excitation pathways and signifies $\chi = 0$ at a certain probe frequency for a given choice of atom-field interaction parameters. For $\Omega_1 \gg \Omega_2$ and $\Delta_1 = 0$, (1) and (2) predict two symmetric ($\Delta_2 = \pm\Omega_1/2$) AT resonances of equal line width and a narrow transmission signal (EIT) at $\Delta_2 = 0$. EIT may also be observed for $\Delta_1 \neq 0$, but the contrast is generally observed to be poor. Under the matched resonance ($\Delta_1, \Delta_2 = 0$) case the line width of EIT is the narrowest. In this case the Doppler shifts of the pump and probe lasers exactly cancel each other [13, 18] and that gives rise to an enhanced two-photon resonance condition whose frequency position is fixed for all velocity group of atoms. In this situation only the coherent dephasing, which is a combination of spontaneous decay rates and is zero for an ideal Λ system [16], determines S/N ratio of the resulting EIT signal. Exact cancellation of Doppler shifts does not happen in case of $\Delta_1 \neq 0$, which leads to partial or full obscurity of EIT signal due to encroachment by the neighboring AT components on the transparency window. The altogether different origin of EIT compared to AT signal compels us to reinvestigate the atomic frequency offset locking scheme referenced to EIT and sub-Doppler dressed level signal as two different discriminators.

In the domain of atomic frequency offset locking scheme, the probe laser frequency control loop can be thought of as a complicated extension (*cf.* Fig. 2) of ordinary closed loop application of laser. Following the schematic illustration by T. Day et al. [19] we may write the frequency noise spectral density $S_{\Delta\nu}(f)$ of the offset locked probe laser as

$$S_{\Delta\nu,\text{cl,offsetlock}} = \frac{\sqrt{S^2_{\Delta\nu,\text{laser}} + S^2_{\Delta\nu,\text{transferred}}}}{|1 + H(f)|}, \tag{3}$$

where $S_{\Delta\nu,\text{cl,offsetlock}}(f)$ is the frequency noise power of the coupled laser, $H(f)$ is the transfer function of the feedback loop, $S_{\Delta\nu,\text{laser}}(f)$ is the noise power of the probe laser itself and $S_{\Delta\nu,\text{transferred}}(f)$ is the noise introduced by the pump laser to the probe laser feedback loop (*cf.* Fig. 2). It may be noted here that the time evolution of laser frequency stability is based on the statistical averaging of the frequency fluctuations. Therefore, the systematic errors, e.g. shift of the pump laser lock point, and the random errors, e.g. flicker noise in the pump laser, will contribute to probe laser lock stability in

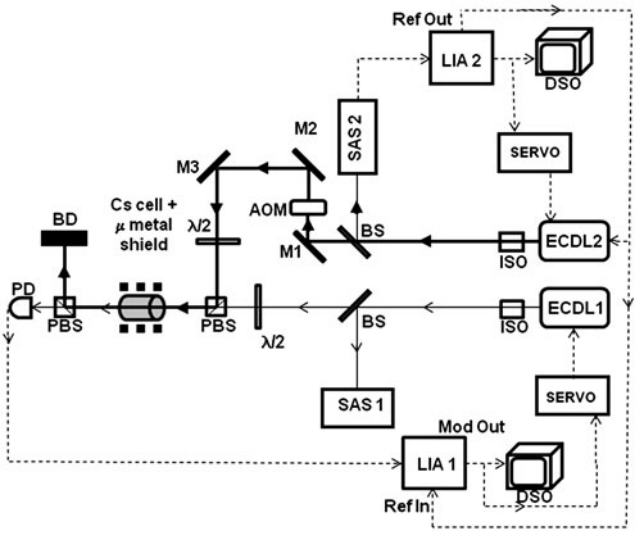

Fig. 3 Schematic of the experimental arrangement. *ECDL*: external cavity diode laser, *M*: mirror, *BS*: beam splitter, *ISO*: isolator, *BD*: beam dump, *PD*: photodetector, $\lambda/2$: wave plate, *LIA*: lock-in amplifier, *AOM*: acousto optic modulator, *DSO*: digital storage oscilloscope and *SAS*: saturation absorption setup. For EIT the *rf* power to AOM is turned off so that the un-deflected pump beam can pass through the vapor cell. For sub-Doppler AT signal the AOM is turned on and the first order (+1) is made to co-propagate with pump beam by small adjustment of *M2*, *M3*. Probe (pump) laser is *ECDL1* (*ECDL2*)

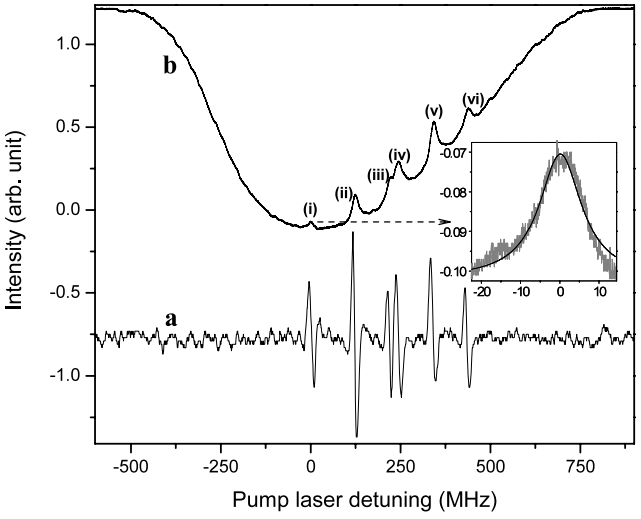

Fig. 4 Simultaneous recording of (**a**) third derivative signal of (**b**) pump laser SAS spectrum. In (**b**) the resonances (i, iv, vi) correspond to $F = 4 \rightarrow F' = 5, 4, 3$ and (ii, iii, v) are the appropriate crossover transitions. *Inset* shows Lorentzian fit of the resonance (i). The FWHM is 13 MHz

addition to the probe laser's own noise. As a consequence of $S_{\Delta\nu,\text{transferred}}(f)$, the servo system starts to write the pump laser noise on the probe laser system and that points to a situation where the pump laser becomes the key factor in determining the stability of the probe laser. Note here that (3) is constructed by assuming $S_{\Delta\nu,\text{laser}}(f)$ and $S_{\Delta\nu,\text{transferred}}(f)$ are in quadrature. This assumption is made for the sake of presenting simplified expression (*cf.* (3)) representing the noise power spectrum of the offset locked laser. Actual situation may be more complex for such coupled laser system. However in an atomic frequency offset locking scheme the pump laser is linked to probe laser via coherence (*cf.* (1)) and the situations are quite different for discriminators based on dressed level resonance and EIT resonance, as has been discussed above. This forbids us to draw any general conclusion on the stability of the probe laser, which is locked to EIT and sub-Doppler dressed level signal in the line of conventional frequency offset locking.

3 Experimental scheme

The experimental set-up used for obtaining narrow AT as well EIT signals and further for frequency offset locking is shown schematically in Fig. 3. Two external cavity tunable diode lasers are used as the probe (ECDL1) and pump (ECDL2) lasers. Optical isolators (isolation 30 dB) are used before the lasers to prevent optical feedback. Typical values of Ω_1 and Ω_2 used in the experiments are ∼25 MHz and ∼5 MHz respectively. A very small part (∼100 μW) of each laser is used to obtain saturated absorption spectrum (SAS) of the relevant transitions. To estimate the line width, both lasers are independently tuned to the slope of SAS of the hyperfine transition $6s_{1/2}F = 4 \rightarrow 6p_{3/2}F' = 5$ for frequency discrimination. The SAS spectrum obtained with pump laser for example is shown in Fig. 4. It is very nearly Lorentzian with full width at half maximum (FWHM) of ∼13 MHz. The observed SAS line width is mainly limited by power broadening (∼11.3 MHz) of natural line width and optical misalignment (∼1.5 MHz) as revealed by theoretical estimate. Instrumental broadening, which is largely dominated by laser line width, is another dominant contributor of the SAS line width. To estimate instrumental broadening the laser is left in the free running mode after reaching the linear part of the discriminator slope. Such a spectroscopic discriminator is less susceptible to the mechanical or acoustic disturbance [20] and hence useful in proper calibration of frequency fluctuations. The laser frequency deviation (error signal), which is recorded at a speed of 100 k Samples/s with a digital storage oscilloscope (DSO) is shown in the inset of Fig. 5 together with its frequency noise power spectral density $S_{\Delta\nu}(f)$ in Fig. 5. It can be seen that main contribution to $S_{\Delta\nu}(f)$ is contained in the Fourier frequency (f) range of 10 kHz. The rms line width $(\Delta\nu_{\text{rms}})$ of the laser system is given by [21]

$$\Delta\nu_{\text{rms}}^2 = 2\int_0^\infty S_{\Delta\nu}(f)df \tag{4}$$

Here $\Delta\nu_{\text{rms}}$ is ∼400 kHz within the limit of $f_{\max} =$ 50 kHz. By assuming the noise present in the laser sys-

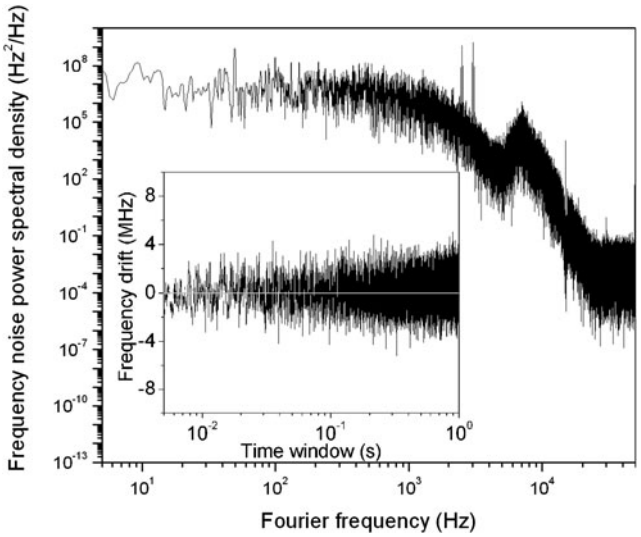

Fig. 5 Frequency noise power spectrum of the free running laser $S_{\Delta\nu,\text{laser freerunning}}$ vs. Fourier frequency (f). Area under the curve corresponds to $\Delta\nu^2_{\text{rms}}$ i.e. square of the rms line width of the laser. The *inset* shows short-term frequency fluctuations of the ECDL recorded over 1 s time window with sampling speed of 100 k Samples/s. The laser is left free running after reaching the slope of SAS of $F = 4 \rightarrow F' = 5$

tem is Gaussian in nature [22], the practical line width $\Delta\nu(2.35\Delta\nu_{\text{rms}})$ is ∼1 MHz and it represents the convolution between the spontaneous line width of the laser and the technical noise present in the laser. It sets the limit of the frequency resolution that the ECDL system can attain during the scan. In the present case the practical laser line width is lower than the natural line width of the D_2 transition of Cs (5.3 MHz).

In Fig. 3 the pump and probe laser beams are orthogonally plane polarized. A polarizing cubic beam splitter (PCBS) is used to make these two beams collinear and propagate through a Cs vapor cell of ∼3 cm length. The cell is maintained at room temperature (22°C) and wrapped with μ-metal shield to reduce the effect of ambient magnetic field. After exiting from the cell the pump and probe laser beams are separated by use of another PCBS and the probe beam is detected on a photodetector. The isolation obtained with the PCBS is > 40 dB. For obtaining sub-Doppler dressed level absorption signals the pump is locked to $6S_{1/2}F = 4 \rightarrow 6P_{3/2}F' = 5$ transition with the help of frequency modulation spectroscopy (FMS) and further blue detuned by 110 MHz using an AOM, thereby achieving detuning $\Delta_1 = -560$ MHz with respect to the transition $6s_{1/2}F = 4 \rightarrow 6p_{3/2}F' = 3$. In case of EIT the pump laser is locked to $6s_{1/2}F = 4 \rightarrow 6p_{3/2}F' = 3$ transition. In both these experiments the probe laser is scanned across $F = 3 \rightarrow F' = 2, 3, 4$ to complete the driven Λ system. The FMS of pump laser is done by third harmonic detection with the help of a lock-in amplifier (LIA1). For this purpose the pump laser current is modulated with a sine wave (frequency 10 kHz and pk–pk amplitude of 10 mV). This introduces frequency excursion of $\sim \pm 1$ MHz (as calculated from current tuning rate of the pump laser), which is equivalent to the unperturbed line width of the laser. Hence the effect of modulation on the pump laser absorption spectrum is negligible. Similar FMS is done for the probe laser, however the probe laser is not directly modulated. The modulation transfer [9] from the pump to the probe laser takes place by the coherent coupling (*cf.* (1)). This situation removes the possibility of affecting probe laser line width that may arise due to direct modulation. We used a ramp (1 Hz) to sweep the probe laser frequency. As a result the EIT and sub-Doppler absorption signal is scanned within a time window of ∼1 and 5 ms. Under this condition the probe laser spectrum is limited by the practical line width of ∼1 MHz. The modulation signal, which is used for modulating the pump laser, is also used at the reference input of the lock-in amplifier (LIA2) extracting third derivative signal of the probe laser absorption spectrum. The low pass filter time constant at the lock-in amplifier output is set at 1 ms for all three cases.

The choice of third derivative discrimination signal over the first derivative in laser frequency control has distinct advantage. In case of first derivative signal the background of the signal may contain gain vs. frequency response of the laser itself. This is a serious problem with diode lasers because of strong interrelation between intensity and frequency. In particular the presence of background intensity slope results in the shift of the lock point (i.e. zero voltage of the LIA output) and as a consequence the servo system requires an additional stable offset to compensate for the shift in lock point from the zero reference. In this situation the stability performance of the diode laser is critically determined by the stability of the offset voltage. A better alternative is to lock on the third derivative feature where the background intensity fluctuations get nullified and the zero voltage output of the LIA faithfully represents the peak of the spectral feature. However high sensitivity of the third derivative detection technique can be availed at the cost of high modulation amplitude applied to the laser frequency. Though by using modulation transfer technique we avoid direct modulation of the probe laser, the effect from pump laser modulation is clearly evident in Fig. 5 where the third derivative signal is broadened (peak to peak excursion ∼5 MHz) compared to original EIT signal (line width ∼2 MHz). However the present experiment is aimed at drawing a general conclusion about the stability of atomic frequency offset locking where the principal requirement is to remove effect of diode laser intensity fluctuations from the measurement so that the study can be focused in the domain of laser frequency noise. Third harmonic locking can only provide this opportunity and therefore it is followed here.

The frequency stabilization of the probe on discriminator signal is done by introducing a correction signal to the piezo

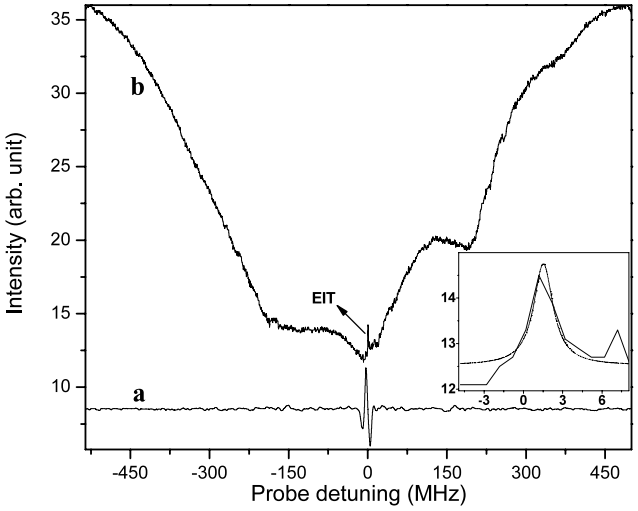

Fig. 6 Simultaneous recording of (**a**) third derivative signal of (**b**) EIT. The pump laser is locked at the peak of $F = 4 \rightarrow F' = 3$ hyperfine component. The *inset* shows a Lorentzian fitting of the EIT signal (*dotted line*) of FWHM ∼2 MHz

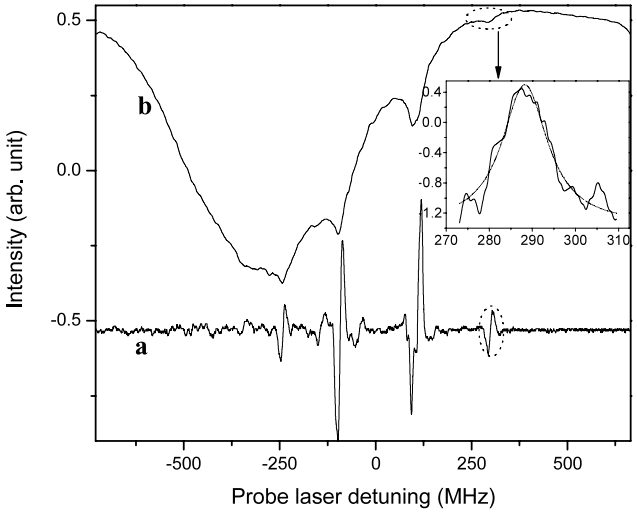

Fig. 7 Simultaneous recording of (**a**) third derivative signal of (**b**) dressed levels when the pump laser is locked at the peak of $F = 4 \rightarrow F' = 5$ hyperfine transition and further blue detuned by 110 MHz using AOM. Sub-Doppler features on the probe absorption spectrum (**b**) appear due to formation of Λ driven coherence between $F = 4,3 \rightarrow F' = 4$ and $F = 4,3 \rightarrow F' = 3$ as initiated by the far blue detuned pump laser. The resonance (highlighted) outside Doppler profile is used for frequency locking. The inset shows a Lorentzian fitting of the sub-Doppler absorption signal of FWHM ∼10 MHz

actuator. The total response bandwidth of the piezo actuator is 1 kHz. The zero point of the third derivative discriminator signal is selected as the lock point and is processed through a proportional-integrator (PI) control loop. The open loop corner frequency (3 dB) of the PI loop is ∼600 Hz, which matches well with the piezo bandwidth. Under the closed loop condition the output of the lock-in amplifier is recorded with a DSO at a sampling speed of 50 k Samples/s. The recorded output is used for further analysis of frequency stability.

4 Results and discussion

The probe absorption spectra are shown in Figs. 4, 6, 7 for the cases of SAS (line width ∼13 MHz), sub-natural EIT (line width ∼2 MHz) and sub-Doppler AT resonance (line width ∼10 MHz) respectively. The slopes of the corresponding third derivative signals are 80 mV/MHz (SAS), 900 mV/MHz (EIT) and 15 mV/MHz (AT). We now focus our attention on the stability of the frequency offset lock using EIT and AT. Here a signal having line width below or in the range of the natural line width serves as a useful discriminator to replicate the master-slave configuration.

In our experiments, we make closed loop measurements of error signal of the individual lasers (ECDL1 and ECDL2) simultaneously. The results of these measurements for SAS, EIT and AT, are shown in Fig. 8. Further we calculate the square root of Allan variance $\sigma(2, \tau)$ from subsequent FFT analysis of error signal, as depicted in Figs. 9 and 10. We now focus on the case by case study of laser frequency stability performance. It may be noted here that the pump laser (ECDL2) is locked to the third derivative signal of $F =$

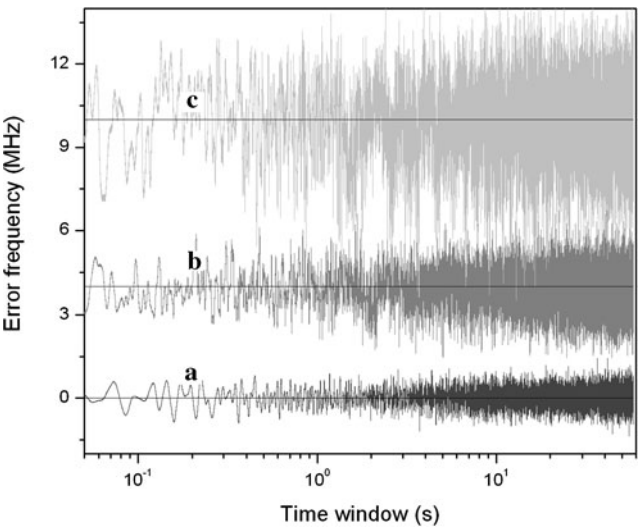

Fig. 8 Simultaneous recording of error signal of (**a**) EIT locked, (**b**) SAS locked and (**c**) sub-Doppler AT signal locked conditions. The $pk \leftrightarrow pk$ frequency excursion of (**a**), (**b**) and (**c**) are ∼1.5 MHz, 3 MHz and 5 MHz respectively. Error frequency magnitude of SAS lock (**b**) is in the order of EIT line width (2 MHz). Further increment in SAS locked error magnitude considerably distorts EIT locking condition as observed in the experiment. For SAS lock error magnitude ∼EIT line width, the EIT system performs better (see text for details). However, no such correlation can be thought of between (**b**) and (**c**)

$4 \rightarrow F' = 3$ and $F = 4 \rightarrow F' = 5$ hyperfine components for observation of EIT and sub-Doppler AT resonance respectively. The pump laser frequency stability in both of these

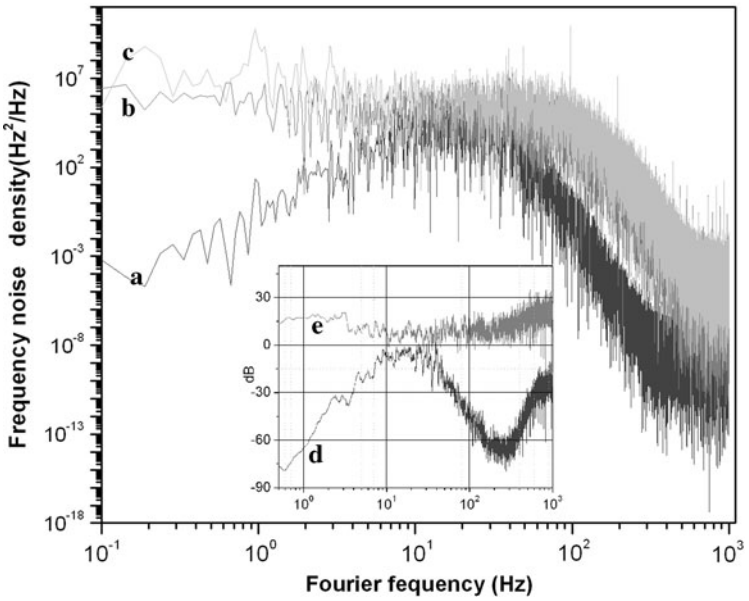

Fig. 9 Frequency noise power spectral density for probe laser under (**a**) EIT lock and (**c**) sub-Doppler AT lock. The frequency noise power density of the pump laser under SAS lock is given by (**b**). In the *inset* (**d**) and (**e**) respective show the plots of $10\log(S_{\Delta\nu,\text{EIT lock}}/S_{\Delta\nu,\text{SAS lock}})$ vs. f and $10\log(S_{\Delta\nu,\text{AT lock}}/S_{\Delta\nu,\text{SAS lock}})$ vs. f. The EIT locked system always grazes below the noise floor of SAS locking while the opposite is seen for sub-Doppler AT locking (see text for details)

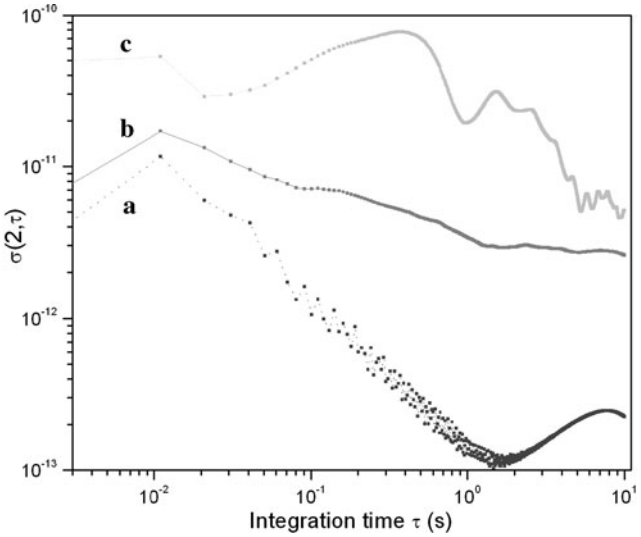

Fig. 10 Comparison of square root of Allan variance (σ) for (**a**) EIT lock, (**b**) SAS lock and (**c**) sub-Doppler AT lock conditions. The result is in tune with the inference drawn from FFT analysis. After $\tau = 10$ s $\sigma(2,\tau)$ attain a value of (**a**) 2×10^{-13}, (**b**) 2×10^{-12} and (**c**) 6×10^{-12}

situations yields similar results. Henceforth we generalize pump laser frequency stability as frequency stability of SAS lock without distinguishing between $F = 4 \rightarrow F' = 3{,}5$ references.

Figure 8 shows lowest pk–pk error frequency fluctuations ($\Delta\nu$) of ~1.5 MHz for EIT locking and highest (~5 MHz) for sub-Doppler AT locking. The SAS locking produces intermediate result of error frequency fluctuations (~3 MHz). Note here that the pump laser current modulation amplitude ~10 mV remains same throughout the experiment. Similar results are obtained for FFT spectra (Fig. 9), which clearly shows the probe laser under EIT lock produces least frequency noise compared to SAS locked pump or AT locked probe laser. We calculate $10\log(S_{\Delta\nu}(f)_{\text{EIT(AT) lock}}/S_{\Delta\nu}(f)_{\text{SAS lock}})$ (dB) to show the relative stability of the probe laser with respect to that of the pump (*cf.* Inset of Fig. 9). Here also the $S_{\Delta\nu}(f)_{\text{EIT lock}}$ always grazes below the $S_{\Delta\nu}(f)_{\text{SAS lock}}$ (maximum −70 dB at $f = 150 \rightarrow 380$ Hz). On the contrary the $S_{\Delta\nu}(f)_{\text{AT lock}}$ remains at par or above $S_{\Delta\nu}(f)_{\text{SAS lock}}$ (maximum 25 dB at $f = 500$ Hz onwards). Overall study of $S_{\Delta\nu}(f)$ vs. f (Fig. 9) reveals that $S_{\Delta\nu}(f)_{\text{EIT lock}}$ is considerably less than $S_{\Delta\nu}(f)_{\text{SAS lock}}$ within $f = 10$ mHz $\rightarrow$ 20 Hz and 40 Hz $\rightarrow$ 1 kHz regions. This indicates both short and long-term stability of the EIT locked probe laser is better in comparison with the pump laser. However $S_{\Delta\nu}(f)_{\text{AT lock}} \geq S_{\Delta\nu}(f)_{\text{SAS lock}}$ as is observed throughout the FFT range ($f = 10$ mHz $\rightarrow$ 1 kHz).

It can be seen in Fig. 9 that within $f = 20 \rightarrow 40$ Hz pump and probe laser noise become near equivalent for both EIT and AT locked conditions. To explain this we may point out that unlike SAS or AT signal, large EIT discriminator slope induces significant enhancement in integral (I) gain even under normal laboratory noise environment leading to instability in the feedback loop. In order to avoid this situation an additional loop filter is introduced to slowly roll off the I gain so that the feedback response becomes increasingly proportional (P) beyond $f \sim 20$ Hz. At $f > 40$ Hz the noise suppression is jointly done by the P control and the LIA. Same feedback network is used for SAS and AT lock. Since the frequency control within $f = 20 \rightarrow 40$ Hz is principally proportional in nature, the stability of EIT locked laser stays in close proximity (average 5 dB below zero line i.e. $S_{\Delta\nu}(f)_{\text{SAS lock}}$ within $f = 20 \rightarrow 40$ Hz) with the AT or SAS locked condition. It may be noted that the

modified feedback strategy decreases the open loop bandwidth of the servo. However it ensures mutual comparison of all the frequency references under similar feedback gain $|\mathbf{1} + H(f)|^{-1}$ environment, which is the main objective of the present study.

We calculate $\sigma(2,\tau)$ on the basis of numerical integration [23–25] as shown below:

$$\sigma^2(2,\tau) = \frac{2}{\nu_0^2}\int_0^\infty S_{\Delta\nu}(f)\frac{\sin^4(\pi f\tau)}{(\pi f\tau)^2}\,df, \tag{5}$$

where τ is integration time and ν_0 is the nominal frequency (3.518×10^{14} Hz). Figure 10 shows the behavior of $\sigma(2,\tau)$ vs. τ for the pump laser (SAS stabilized) and probe laser stabilized on AT and EIT references. It is observed that at $\tau = 10$ s the EIT locked probe laser attains a minimum of $\sigma \sim 2.0 \times 10^{-13}$ whereas the pump laser shows $\sigma \sim 2.4 \times 10^{-12}$. However the pump laser stability betters than that of the AT locked probe laser, which shows $\sigma \sim 6.2 \times 10^{-12}$ at $\tau = 10$ s. This situation shows that stability measurements in atomic frequency offset locking scheme under EIT reference can contravene the expected outcome of conventional Master-Slave offset locking. On the contrary the behavior of a laser referenced to the dressed level transition (AT resonance) reveals the fact that the pump laser sets stability limit of the probe laser. This is in accordance with the theme of conventional Master-Slave offset locking scheme. Note here that the closed loop method of analyzing frequency stability actually represents lower limit of Allan variance because it does not consider the noise of the discriminator [19, 25]. However the error signal is weighted by servo loop transfer function, so in principle it is possible to extract laser frequency stability from the error signal [24]. Despite of this limitation the closed loop method can effectively explore the relative frequency stability of the laser.

We now discuss the contrasting nature of the atomic frequency offset locking referenced to EIT and AT resonance as observed in Figs. 8, 9 and 10. In short integration time scale (τ), EIT lock is expected to perform better than the AT lock since the laser frequency stability is principally dominated by the steepness of the slope ($d\nu/dV$) of the discriminator signal, which is 900 mV/MHz and 15 mV/MHz for EIT and AT respectively. However under relatively longer averaging time the frequency error accumulated for the probe laser is more susceptible to noise because of the coherently established correlation with the pump laser.

It is evident from (1) that the pump laser parameters Δ_1 and Ω_1 directly influence the coherent coupling. However the situations are dramatically different for EIT and AT. In this context, we is instructive to refer to the work of Javan et al. [26] which gives the FWHM of EIT line width ($\Gamma_{\rm EIT}$) as

$$\Gamma_{\rm EIT} = \Omega_1\left[\frac{\Gamma_{13}}{\Gamma}(1+x)\left(1+\left(1+\frac{4x}{(1+x)^2}\right)^{1/2}\right)\right]^{1/2} \tag{6}$$

where $\Gamma = \Gamma_{13} = \Gamma_{12}$ is the natural line width, Γ_{13} is the non-radiative decay between the dipole forbidden hyperfine levels $|1\rangle$ and $|3\rangle$, $x = \Omega_1^2\Gamma/2\Gamma_{13}D^2$ and D is the Doppler width of the atomic medium. In the analysis that follows we assume that Γ_{13} is decided by transit time broadening [24] and obtain $\Gamma_{13} \sim 20$ KHz for our experimental configuration. For the range of experimental parameters in our work, we have $x \leq 1$ and that according to (6) gives

$$\Gamma_{\rm EIT} \sim \Omega_1\left(\frac{2\Gamma_{13}}{\Gamma}\right)^{1/2} \tag{7}$$

Physically it means that $\Gamma_{13}\Gamma \ll \Omega_1^2 \ll D^2$ is satisfied and the optical pumping rate is given by Ω_1^2/Γ. Using (7) we calculate $\Gamma_{\rm EIT} \sim 4$ MHz which compares favorably with the observed line width of ~2 MHz in our experiment. We thus observe that for exact resonance ($\Delta_1 \approx 0$) the line width of the EIT discriminator is independent of Δ_1 and is a function of pump intensity alone. This is different from the line width of AT signal (*cf.* (2)), which is strongly dependent on both Δ_1 and Ω_1. Now consider the situation where the SAS stabilized pump laser fluctuates about the lock point. Figure 8 shows pk–pk $\Delta\nu_{\rm pump} \sim$ 3 MHz, which is in the order of the EIT line width. For such small pump frequency fluctuations the EIT condition $\Omega_1^2\Gamma/(\Gamma^2 + \Delta\nu_{\rm pump}^2) \gg \Gamma_{13}$ is still well satisfied. Here $\Omega_1^2\Gamma/(\Gamma^2 + \Delta\nu_{\rm pump}^2)$ is the revised optical pumping rate [26, 27], which drops to $(\Omega_1^2/2\Gamma)$ when $\Delta\nu_{\rm pump} \sim \Gamma$ but still remains much greater than Γ_{13}. Intuitively we can conclude that even if the peak locked pump laser suffers frequency fluctuations of the order of Γ, the $\chi \to 0$ condition within narrow EIT window remains undisturbed due to strong optical pumping. As a result the signature of EIT, which is a non-absorptive resonance, is still well preserved and its line width becomes independent of $\Delta\nu_{\rm pump}$. We may therefore conclude that $S_{\Delta\nu}(f)_{\rm EIT\ lock}$ is a weak function of $S_{\Delta\nu}(f)_{\rm transferred}$ (see (3)). Figure 8 also shows $\Delta\nu_{\rm prob,EIT\ lock} \sim 1.5$ MHz, which supports weak pump error frequency dependence of EIT locked probe laser. The sub-Doppler AT resonance, which is an absorptive resonance, appears with a finite value of χ and its width is strongly dependent on Δ_1. It means that even the pump laser frequency fluctuates to any small extent so does the probe laser referenced at dressed signal making the contribution of $S_{\Delta\nu}(f)_{\rm transferred}$ crucial in the probe laser stability. This subtle difference in the origin of EIT and AT resonance is the main reason behind the opposite behavior of two different atomic frequency offset locking references though both spectral features can be obtained as results of pump-probe spectroscopy carried out in a coherently prepared atomic medium. We may add here that the superior performance of the EIT lock can continue as long as $\Delta\nu_{\rm pump}$ does not deteriorate the optical pumping rate drastically. For $\Delta\nu_{\rm pump} > \Gamma$

the optical pumping rate falls rapidly, e.g., $\Delta\nu_{\text{pump}} \sim 3\Gamma$ (in the range of SAS line width) the optical pumping falls to 10% of Ω_1^2/Γ, rendering degraded performance of EIT locked laser system because $\chi \to 0$ condition gets increasingly obscured by the background absorption.

The other issue of concern is the modulation transfer in the pump-probe experiments. Variation in magnitudes of slopes in case of EIT and AT resonances also indicates different degree of modulation transfer for fixed modulation amplitude of the pump laser. In this connection we may borrow the conclusions of Xiao et al. [28]. The modulation transfer function $T(\omega_{\text{mod}})$ is a function of residual Doppler width (δD) and Γ_{13}. While Γ_{13} is same for both atomic frequency offset locking schemes, δD is zero for EIT and is finite for AT signal. In case of Rb D_1 transition Xiao et al. [28] clearly showed that the switching speed in EIT kind of system is limited by δD. Here smaller values of δD favors higher modulation transfer amplitude. It is to be noted that extraction of derivative signal in FMS typically depends on modulation depth. By comparing the third derivative signatures of EIT and sub-Doppler signal (for a fixed pump modulation) it can clearly be concluded that modulation transfer is more in case of EIT than the sub-Doppler AT signal. Hence derivative signal of EIT is obtained with higher (S/N) ratio than the AT signal.

5 Conclusion

In this work we have addressed the issue of frequency stability in atomic frequency offset locking scheme with two independent lasers. For this purpose the coherent pump-probe spectroscopy of Cs atom in Λ configuration is conducted. Unlike some of the previous reports [10, 12], where the emphasis was more on reducing the line width of the EIT or dressed state transitions to near or below natural line width, the focus in this paper is to investigate the stability of a probe laser (particularly in a relatively moderate integration time scale of ms $\to$ few seconds) that uses sub-natural EIT ($\sim$2 MHz) and sub-Doppler AT resonance ($\sim$10 MHz) as frequency discriminator. The frequency stability is analyzed in terms of Allan variance (σ^2). It has been found that performance of the EIT locked ($\sigma \sim 2 \times 10^{-13}$) laser system is better than the SAS locked pump laser ($\sigma \sim 2 \times 10^{-12}$). This result, though contradicts usual outcome of usual Master-Slave offset locking, is in accordance with the earlier work by Moon et al. [9]. However, a laser locked on sub-Doppler dressed signal reference is inferior ($\sigma \sim 6 \times 10^{-12}$) in stability compared to the pump laser and this result is in tune with the idea of conventional Master-Slave configuration. To understand the peculiar nature of EIT locking we take into account the behavior of susceptibility (χ) in the coherently prepared atomic medium under two-photon resonance condition. In case of EIT $\chi \to 0$ indicates absorption reduction at the cost of enhancement in two-photon resonance. This condition makes the EIT locked laser system literally immune to small pump laser frequency fluctuations, i.e., $\Delta\nu_{\text{pump}} \sim \Gamma_{\text{EIT}}$. In such a situation $\chi(\Delta_1 \approx 0) \to 0$ condition does not effectively change and the EIT line width becomes a function of pump beam intensity alone. However for $\Delta\nu_{\text{pump}} > \Gamma$, the condition $\chi \to 0$ may not remain valid and that may result in smearing out of EIT signal due to encroachment by neighboring AT components. Unlike EIT, the AT resonance is an absorptive signal due to finite value of χ and is sturdily controlled by pump laser parameters. This physical insight helps us to conclude that though the EIT and AT signals are results of coherent pump-probe spectroscopy, they behave differently when used as frequency references. We strongly believe different role played by susceptibility of the medium for absorptive and non-absorptive resonances is the reason behind superior performance of EIT locked system. In the same tune we can also conclude that non-absorptive optical resonance (like EIT) is always a better choice as frequency discriminator than absorptive resonances (like SAS, AT etc.).

We may also add here that it is possible to obtain the AT resonance of sub-natural line width [12–14] by dressing the atomic system with a pump laser of sufficiently large blue detuning. However such large blue detuning of pump frequency produces weaker signal with lower S/N and that makes it difficult to retrieve a workable frequency discriminator signal. Even that were possible, we strongly believe that the result of frequency stabilization will remain same as ours. Also there may arise a question about the performance of a probe laser if stabilized on an AT frequency reference within Doppler profile [12]. The result will remain unaltered since the generic equation (*cf.* (2)) is always same for AT resonance irrespective of its appearance within or outside Doppler profile.

Acknowledgements Y.B. Kale personally thanks the DAE—University of Mumbai collaboration for granting a research fellowship. Y.B. Kale and A. Ray acknowledge the support from Dr. A.K. Das, Head, L&PTD and Dr. L.M. Gantayet, Director, BTDG, during the work.

References

1. E. Arimondo, *Progress in Optics*, vol. XXXV (Elsevier Science, Amsterdam, 1996), p. 258
2. K.J. Boller, A. Imamoglu, S.E. Harris, Phys. Rev. Lett. **66**, 2593 (1991)
3. R. Wynands, A. Nagel, Appl. Phys. B **68**, 1 (1999)
4. I. Mazels, B. Matisov, E. Cerboneschi, E. Arimondo, Phys. Lett. A **229**, 77 (1997)
5. S. Harris, Phys. Rev. Lett. **62**, 1033 (1989)
6. J. Kitching, S. Knappe, N. Vukičević, L. Hollberg, R. Wynands, W. Weidmann, IEEE Trans. Instrum. Meas. **49**, 1313 (2000)

7. S. Knappe, V. Shah, P.D. Schwindt, L. Hollberg, J. Kitching, L. Liew, J. Moreland, Appl. Phys. Lett. **85**, 1460 (2004)
8. M. Stähler, S. Knappe, C. Affolderbach, W. Kemp, R. Wynands, Europhys. Lett. **54**, 323 (2001)
9. H.S. Moon, L. Lee, K. Kim, J.B. Kim, Appl. Phys. Lett. **84**, 3001 (2004)
10. S.C. Bell, D.M. Heywood, J.D. White, J.D. Close, R.E. Scholten, Appl. Phys. Lett. **90**, 171120 (2007)
11. M. Klein, M. Hohensee, Y. Xiao, R. Kalra, D.F. Phillips, R.L. Walsworth, Phys. Rev. A **79**, 053833 (2009)
12. U.D. Rapol, A. Wasan, V. Natarajan, Phys. Rev. A **67**, 053802 (2003)
13. Y. Zhu, T.N. Wasserlauf, Phys. Rev. A **54**, 3653 (1996)
14. J. Wang, Y. Wang, S. Yan, T. Liu, T. Zhang, Appl. Phys. B **78**, 217 (2004)
15. K. Kuboki, M. Ohtsu, IEEE J. Quantum Electron. **QE-23**, 388 (1987)
16. D.J. Fullton, S. Shepherd, R.R. Moseley, B.D. Sinclair, M.H. Dunn, Phys. Rev. A **52**, 2302 (1995)
17. J. Gea-Banacloche, Y. Li, S. Jin, M. Xiao, Phys. Rev. A **51**, 576 (1995)
18. G. Vemuri, G.S. Agarwal, B.D. Nageswara Rao, Phys. Rev. A **53**, 2842 (1996)
19. T. Day, E.K. Gustafson, R.L. Byer, IEEE J. Quantum Electron. **28**, 1106 (1992)
20. H. Talvitie, A. Pietiläinen, H. Ludvigsen, E. Ikonen, Rev. Sci. Instrum. **68**, 1 (1997)
21. M. Vainio, M. Merimaa, E. Ikonen, Sci. Technol. **16**, 1305 (2005)
22. D.S. Elliot, R. Roy, S.J. Smith, Phys. Rev. A **26**, 12 (1982)
23. J. Rutman, F.L. Walls, Proc. IEEE **79**, 952 (1991)
24. J.A. Barnes, A.R. Chi, L.S. Cutler, D.J. Healey, D.B. Leeson, T.E. McGunical, J.A. Mullen, W.L. Smith, R. Sydnor, R.F. Vessot, G.M.R. Winkler, IEEE Trans. Instrum. Meas. **IM-20**, 105 (1971)
25. A. Ray, Can. J. Phys. **86**, 351 (2008)
26. A. Javan, O. Korcharovskaya, H. Lee, M.O. Scully, Phys. Rev. A **66**, 013805 (2002)
27. H. Lee, Y. Rostovtsev, C.J. Bednar, A. Javan, Appl. Phys. B **76**, 33 (2003)
28. A.W. Brown, M. Xiao, Phys. Rev. A **70**, 053830 (2004)